An Analysis of Microstrip with Rectangular and Trapezoidal Conductor Cross Sections

C. J. RAILTON, MEMBER, IEEE, AND JOSEPH P. McGEEHAN, MEMBER, IEEE

Abstract —**In this paper, microstrips with both rectangular and trapezoidal cross sections are analyzed by means of the finite-difference time-domain method and results are presented for microstrip both with and without a passivation layer. Where results from other authors are available, good agreement has been found to exist.**

I. Introduction

THE CURRENT trends in microwave monolithic integrated circuits (MMIC's) are toward higher frequencies, higher component densities, and the development of novel components of increasing complexity. A consequence of these trends, made possible by improvements in fabrication technology, is that many of the approximations used in the CAD of microwave circuits are no longer valid. In particular, due to the very narrow strip widths used in MMIC's, the strip thickness, heretofore largely neglected, may be as large as 30% of the strip width. Moreover, because of the occurrence of underetching or electrolytical growth during fabrication, the cross section of the strip is likely to be better approximated by a trapezoid than by a rectangle. It has recently been shown [1] that these effects need to be accounted for if accurate, and therefore reliable, predictions of performance are to be obtained. In contrast to this, the vast majority of published analyses of microstrip have addressed only the situation where the strip thickness is zero, e.g. [2]–[5]. Of the remainder, most are restricted to the case where the strips have rectangular cross section, as described in [6]–[8]. Only very recently has the more general problem of a microstrip with arbitrary cross section been tackled [1], [9].

The finite-difference time-domain (FDTD) technique has been shown to be a very versatile and effective method for a variety of electromagnetic problems, e.g. [10] and [11], and, more recently, it has been successfully applied to simple microstrip discontinuities, e.g. [12]–[15]. To the authors' knowledge this method has not, so far, been applied to a microstrip with nonrectangular cross section, and only in [16] has it been applied to microstrip with finite thickness.

Manuscript received August 29, 1989; revised March 30, 1990.
The authors are with the Centre for Communications Research, Faculty of Engineering, University of Bristol, Bristol, BS8 1TR, United Kingdom.
IEEE Log Number 9036421.

In this contribution, the FDTD method is used to analyze boxed microstrip with both rectangular and trapezoidal cross sections. It is confirmed that the exact shape of the conductor has a marked effect on the effective permittivity of the microstrip. Results using this method are compared to the findings of [9] using the analytically more complicated boundary element method, where very good agreement is observed. The effect of adding a thin passivation layer is also calculated and, what is important for MMIC designs, it is found that such an addition noticeably reduces the effective permittivity of the microstrip.

II. Application of the FDTD Method

The application of the basic FDTD method to planar waveguide structures has been described in several publications [13], [15] and need not be detailed here. There are, however, a number of differences between these published formulations and that used in this contribution which require comment. In [13] and [14] the problem space is theoretically infinite and terminated with an "absorbing" boundary which simulates the effect of an outgoing wave. In [12], [15], and [16], the problem space is closed and terminated with electric or magnetic walls to form a resonant structure. The former method has the advantage that it is possible to characterize the structure under test over a range of frequencies with a single computer run. The latter has the advantage that there is no requirement for absorbing boundaries which, due to their imperfections, can reduce overall accuracy. The latter method is employed in this paper as it is believed to lead to a more efficient implementation.

In [13], no attempt has been made to use a nonuniform mesh or otherwise provide special treatment for the high field variations in the neighborhood of the strip edge. Moreover, in [14] the same authors report that an attempt to use a nonuniform mesh had a detrimental effect on the accuracy of their results. This necessitated their use of a large number of nodes ($30 \times 55 \times 160$) for a uniform thin microstrip. In contrast to this, the results presented herein have been obtained using a highly nonuniform mesh without any such reduction in accuracy having been observed. The ability to use a nonuniform mesh has enabled accurate results to be obtained using a much smaller number of nodes ($12 \times 20 \times 36$) for uniform thin microstrip.

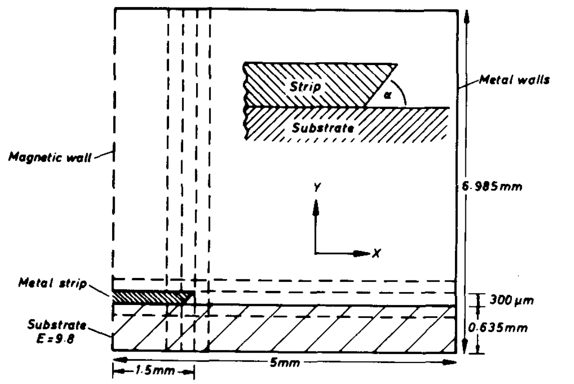

Fig. 1. Microstrip with trapezoidal cross section. Dashed lines show division into regions in the $x-y$ plane.

Fig. 1 shows a typical microstrip structure with trapezoidal conductor cross section. The microstrip is terminated by metal walls in the $x-y$ plane to form a resonator. The dashed lines in the figure show how the mesh is concentrated in the regions of maximum field variation in order to gain good computational efficiency and accuracy. In order to maintain simplicity in programming and to avoid numerical problems, the mesh size is altered independently in the x, y, and z directions even though there will be an unnecessarily high density of nodes in some parts of the box. The right-hand side of the strip which is not orthogonal to the axes has been approximated by a series of small steps.

The form of the initial field is not critical but in order to achieve a steady state as quickly as possible and to concentrate the energy in the dominant mode of the structure, E_y has been given an initial value of $\sin(\pi z/l)$, where l is the length of the microstrip, in the volume under the strip, all other amplitudes being set to zero. The time stepping algorithm is run with the time step being somewhat less than

$$\frac{1}{c\left\{\dfrac{1}{(\min(\delta x))^2}+\dfrac{1}{(\min(\delta y))^2}+\dfrac{1}{(\min(\delta z))^2}\right\}^{1/2}} \tag{1}$$

in order to ensure stability.

Once the time sequence has been obtained, it is multiplied by a raised cosine window function and Fourier transformed. The maximum value of the transformed function gives the resonant frequency of the structure and hence the effective permittivity of the microstrip. It has been found that the time sequence needs to be around 40 cycles long at the resonant frequency in order to get convergence to better than 0.1%. More effective means of extracting the resonant frequency from a shorter sequence are being sought using digital signal processing techniques in order to reduce computation time.

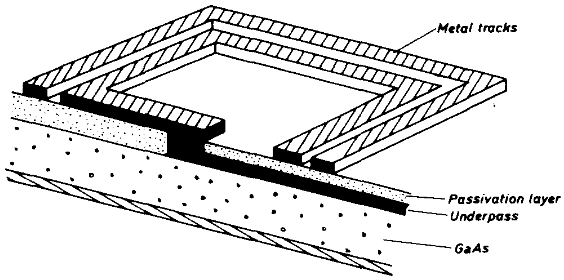

Fig. 2. Cross section of a typical MMIC structure.

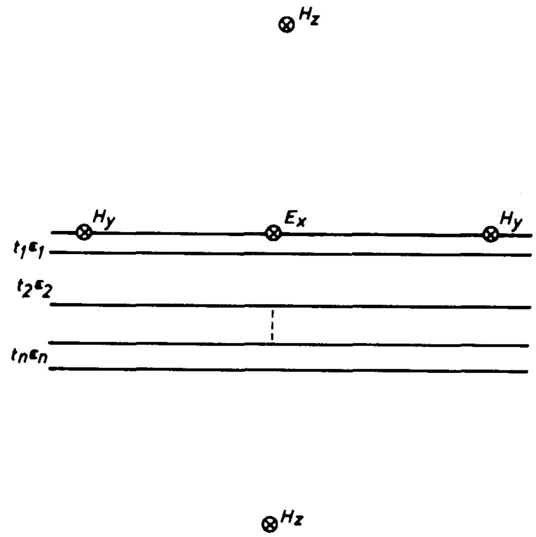

Fig. 3. Cross section of the FDTD mesh in the vicinity of a thin multilayer structure.

III. Incorporation of Layered Dielectrics

A cross section through an MMIC generally reveals a structure of the type shown in Fig. 2. There exists, between the metallization and the GaAs, a very thin passivation layer made from Polyamide having a permittivity in the region of 3.5 and a thickness of the order of 1% that of the GaAs substrate. Due to the large ratio between the thicknesses it is not practicable in the analysis to represent the passivation layer simply by reducing the mesh size. One may, however, make use of the known field boundary conditions at the interface of the substrates in the following way.

For the general case shown in Fig. 3, we have

$$\frac{\partial E_z}{\partial t}=\frac{1}{\epsilon}\left\{\frac{\partial H_y}{\partial x}-\frac{\partial H_x}{\partial y}\right\}-\frac{\sigma}{\epsilon}E_z. \tag{2}$$

Since the gradient $\partial H_y/\partial x$ is assumed constant between the H_x nodes and since E_z is continuous across the dielectric boundaries, we can say, for any pair of adjacent layers i and j,

$$\frac{\partial E_z}{\partial t} = \frac{1}{\epsilon_i}\left\{\left|\frac{\partial H_y}{\partial x} - \frac{\partial H_x}{\partial y}\right|_i\right\} - \frac{\sigma_i}{\epsilon_i}E_z = \frac{1}{\epsilon_j}\left\{\frac{\partial H_y}{\partial x} - \frac{\partial H_x}{\partial y}\bigg|_j\right\} - \frac{\sigma_j}{\epsilon_j}E_z \tag{3}$$

where, in general, the $|_k$ indicates the value of the gradient in layer k and where ϵ_k and σ_k are the permittivity and conductivity of layer k. Rearranging yields

$$\frac{\partial H_x}{\partial y}\bigg|_i = \frac{\epsilon_i}{\epsilon_j}\frac{\partial H_x}{\partial y}\bigg|_j + \left(1 - \frac{\epsilon_i}{\epsilon_j}\right)\frac{\partial H_y}{\partial x} - \left(\sigma_i - \frac{\epsilon_i}{\epsilon_j}\sigma_j\right)E_z \tag{4}$$

and if δH_x is the difference in H_x between the two nodes, we can say

$$\delta H_x = \sum_i d_i \frac{\partial H_x}{\partial y}\bigg|_i \tag{5}$$

where d_i is the thickness of the ith layer.

Letting $j = 1$ in (4) and substituting (5) we get

$$\frac{\partial H_x}{\partial y}\bigg|_1 = \frac{\delta H_x - \frac{\partial H_y}{\partial x}\sum_i d_i\left(1 - \frac{\epsilon_i}{\epsilon_1}\right) + E_z \sum_i d_i\left(\sigma_i - \frac{\epsilon_i}{\epsilon_1}\sigma_1\right)}{\sum_i d_i \frac{\epsilon_i}{\epsilon_1}}. \tag{6}$$

Substituting in (3) we finally get

$$\frac{\partial E_z}{\partial t} = \frac{1}{\epsilon_1}\left\{\frac{\partial H_y}{\partial x} - \frac{\delta H_x - \frac{\partial H_y}{\partial x}P_1 + E_z P_3}{P_2}\right\} - \frac{\sigma_i}{\epsilon_i}E_z \tag{7}$$

where

$$P_1 = \sum_i d_i\left(1 - \frac{\epsilon_i}{\epsilon_1}\right)$$

$$P_2 = \sum_i d_i \frac{\epsilon_i}{\epsilon_1}$$

$$P_3 = \sum_i d_i\left(\sigma_i - \frac{\epsilon_i}{\epsilon_1}\sigma_1\right).$$

This simply requires that (7) be used in place of the usual finite-difference formula when calculating the value of E_z at a dielectric boundary.

In a similar manner a formula may be derived for the values of E_x on the dielectric boundaries.

For the simpler case of an interface between two layers and zero conductivity, such as the air–dielectric interface of standard microstrip, (7) reduces to

$$\frac{\partial E_z}{\partial t} = \frac{\partial H_y}{\partial x}\left\{\frac{1}{\epsilon_1} + \frac{d_2(1 - \epsilon_2/\epsilon_1)}{\epsilon_1 d_1 + \epsilon_2 d_2}\right\} - \frac{2\delta H_x}{\epsilon_1 d_1 + \epsilon_2 d_2}. \tag{8}$$

Furthermore, if $d_1 = d_2 = \delta y$, we get

$$\frac{\partial E_z}{\partial t} = \frac{2}{\epsilon_1 + \epsilon_2}\left(\frac{\partial H_y}{\partial x} - \frac{\partial H_x}{\partial y}\right) \tag{9}$$

TABLE I
REGION SIZES USED FOR TRAPEZOIDAL MICROSTRIP

In the x direction:

Region Number	Region Size ($w = 3$ mm)	Region size ($w = 1.2$ mm)
1	0.9 mm	0.3 mm
2	0.3 mm	0.3 mm
3	0.3 mm	0.3 mm
4	0.3 mm	4.1 mm
5	3.2 mm	

In the y direction:

Region Number	Region Size
1	0.335 mm
2	0.3 mm
3	0.3 mm
4	0.3 mm
5	5.765 mm

In the z direction all regions were one sixth of the resonator length.

TABLE II
REGION SIZES USED FOR INFINITELY THIN MICROSTRIP

In the x direction:

Region Number	Region Size
1	1.25 mm
2	0.50 mm
3	3.25 mm

In the y direction:

Region Number	Region Size
1	0.335 mm
2	0.3 mm
3	0.3 mm
4	0.3 mm
5	5.75 mm

In the z direction all regions are one sixth of the resonator length.

showing that, in agreement with Zhang and Mei [13], it is possible, in this simple case, merely to use the average value of the dielectric constants in the standard finite-difference formulas.

Similar considerations apply to the calculation of the tangential H field if the permeabilities of the material are different.

IV. RESULTS

The structure shown in Fig. 1 was analyzed using a nonuniform mesh with the maximum node density in the areas of maximum field variation. The dashed lines in the figure show the region boundaries. Tables I and II show the sizes of the regions used; each region contains $4 \times 4 \times 4$ nodes. In Fig. 4 the propagation constant of the structure is shown as a function of frequency for an infinitely thin strip and for trapezoidal strips with corner angles, α, of 45° (underetched), 90° (rectangular), and 135° (electrolytic growth). Where available, the results are compared with those obtained by Michalski and Zheng [9], who used the mixed potential integral equation (MPIE) for open microstrip. The results can be seen to be in very good

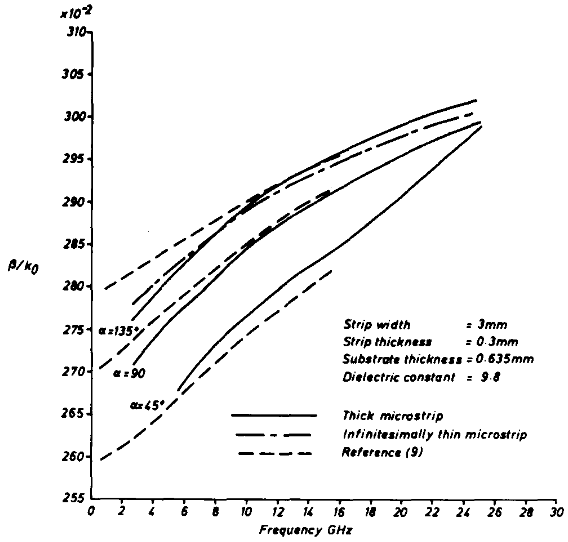

Fig. 4. Propagation constant of microstrip of various cross sections.

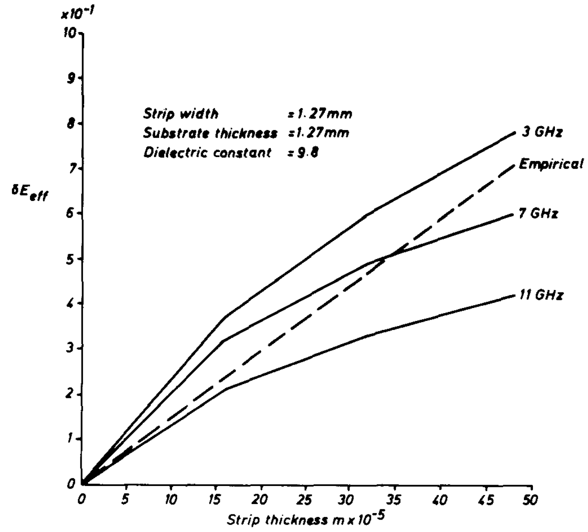

Fig. 6. Variation of effective permittivity with strip thickness.

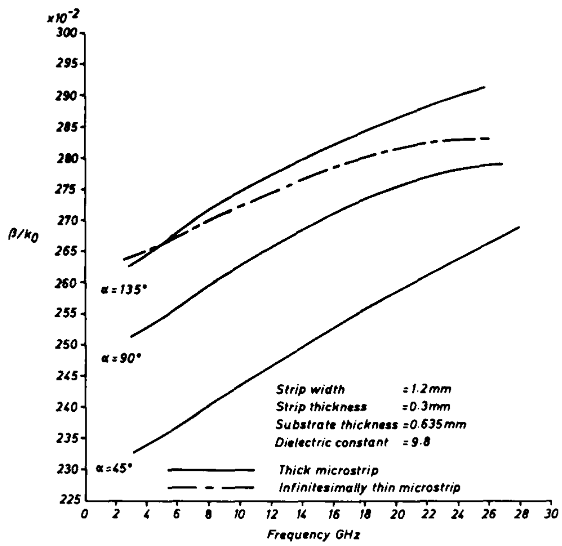

Fig. 5. Propagation constant of microstrip of various cross sections.

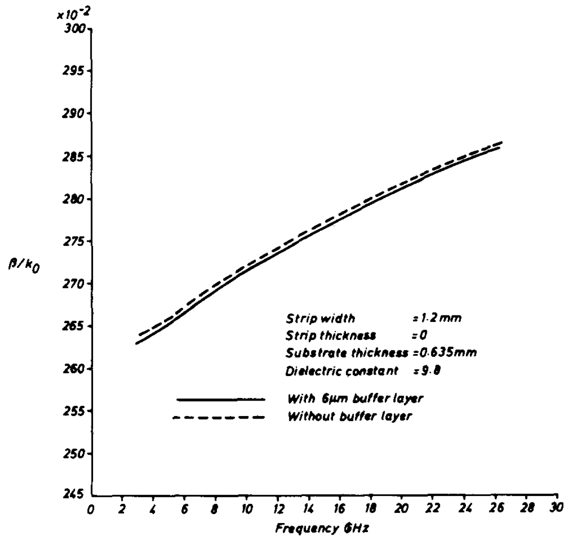

Fig. 7. Propagation constant of microstrip with buffer layer.

agreement. The differences in the results which can be seen at low frequencies would be expected since those from [9] apply to open, rather than boxed, microstrip. Similar results are shown in Fig. 5 for the same geometry but with a strip width of 1.2 mm.

Fig. 6 shows the variation of permittivity with strip thickness for a rectangular strip at a number of frequencies. Also shown, for comparison purposes, is the empirical correction given by Edwards [17]. It can be clearly seen that there is considerable discrepancy between the quasi-static formula and the rigorous solution, especially at large strip thicknesses and at high frequencies. It can also be seen that the effect of finite strip thickness becomes less as the frequency increases. This is in agreement with recently published results [7].

Fig. 7 shows the effect of a thin buffer layer under the metal strip. Exactly the same mesh has been applied as in the case without a buffer layer. It can be seen that the propagation constant is noticeably reduced by even a thin buffer layer.

V. Current Distribution

Significant interest has been shown in the literature concerning the distribution of current in a microstrip. In the work of Uchida *et al.* [18], for example, it is pointed out that there is a disagreement between the currents predicted by different methods. By examining the ***H*** field around the strip predicted by the FDTD method it is

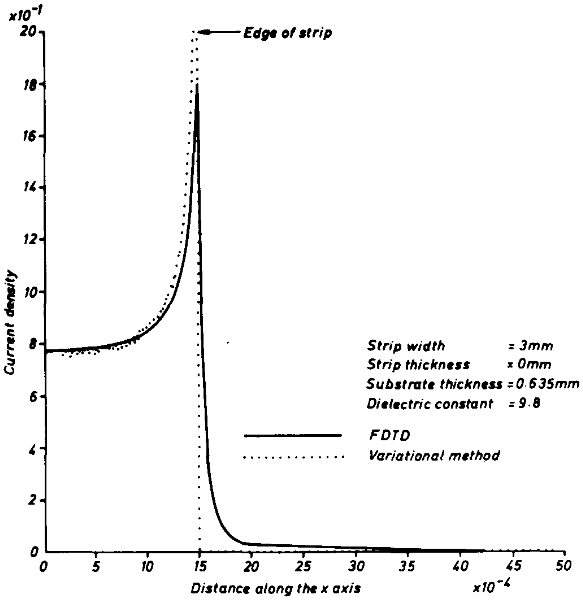

Fig. 8. Longitudinal current in an infinitely thin microstrip.

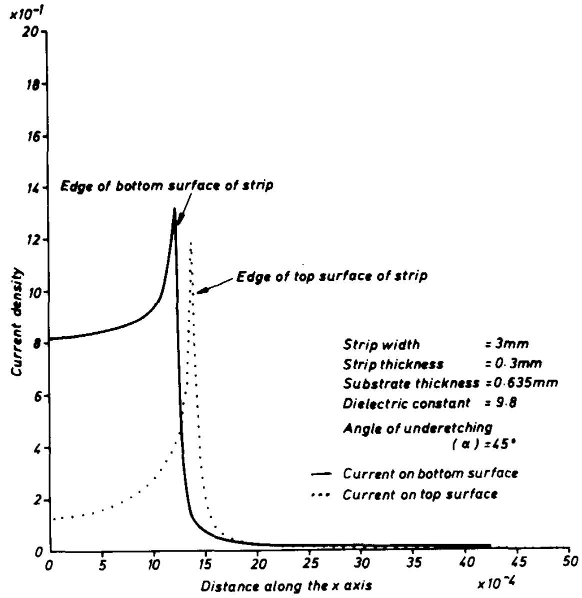

Fig. 9. Longitudinal current in a microstrip with trapezoidal cross section.

possible to calculate the transverse and longitudinal components of current. Fig. 8 shows the longitudinal current predicted by FDTD. The current distribution was also calculated using a variational method [5], with the unknown current expanded in a series of weighted Chebychev polynomials which incorporate a singularity of strength -0.5. It can be seen that the currents predicted by the two methods are almost indistinguishable. Due to the fact that the $\boldsymbol{H}$-field nodes are a finite distance from the interface, there will be a small error in the predicted current. This is evident in the prediction of a finite current density in the region beyond the strip edge, where, in reality, there can be no current. It can be seen, however, that this predicted current is very much less than the real current flowing in the strip. Due to the existence of high-order resonant modes in the FDTD model and the strong dependence of the magnitude of the transverse current on frequency, it is not possible to get an accurate estimate of the transverse current for the dominant mode using the present method.

In Fig. 9 is shown the longitudinal current distributions on the top and bottom of a microstrip with the geometry of Fig. 1 and $\alpha = 45°$ at a frequency of 5 GHz. It can be seen that, as expected, the majority of the current flows on the bottom surface and that singularities exist at the corners.

VI. Conclusion

In this contribution results have been obtained, using the FDTD method, for the effective permittivity of microstrip with rectangular and trapezoidal cross sections with and without a thin passivation layer. The effects of the strip cross section, heretofore largely neglected, must be taken into account if accurate and reliable analyses of modern MMIC structures are required. It has been shown that the FDTD technique is capable of treating microstrip with a general cross section and producing accurate results. Work is proceeding to extend the treatment to discontinuities in microstrip with general cross section.

References

[1] W. Schroeder and I. Wolff, "A new hybrid mode boundary integral method for analysis of MMIC waveguides with complicated cross Section," in *IEEE MTT-S Int. Microwave Symp. Dig.* (Long Beach, CA), 1989, pp. 711, 714.

[2] T. Itoh and R. Mittra, "Technique for computing dispersion characteristics of shielded microstrip lines," *IEEE Trans. Microwave Theory Tech.*, vol. MTT-22, pp. 896–898, Oct. 1974.

[3] N. Fache and D. DeZutter, "Rigorous full-wave space domain solution for dispersive microstrip lines," *IEEE Trans. Microwave Theory Tech.*, vol. 36, pp. 731–737 Apr. 1988.

[4] J. Dekleva and V. Roje, "Accurate numerical solution of coupled integral equations for microstrip transmission line," *Proc. Inst. Elec. Eng.*, vol. 134 pt. H, no. 2, pp. 163–168 Apr. 1987.

[5] C. J. Railton and T. Rozzi, "Complex modes in boxed microstrip," *IEEE Trans. Microwave Theory Tech.*, vol. 36, pp. 865–874 May 1988.

[6] F. Arndt and G. U. Paul, "The reflection definition of the characteristic impedance of microstrip," *IEEE Trans. Microwave Theory Tech.*, vol. MTT-27, pp. 724–731 Aug. 1979.

[7] C. Shih, R. Wu, S. Jeng, and C. Chen, "Frequency dependant characteristics of open microstrip lines with finite strip thickness," *IEEE Trans. Microwave Theory Tech.*, vol. 37, pp. 793–795 Apr. 1989.

[8] S. Tedjini, N. Daoud, D. Rauly, and E. Pic, "Analysis of MMIC's with finite strip thickness and conductivity," *Electron. Lett.*, vol. 24, no. 15, July 1988.

[9] K. A. Michalski and D. Zheng, "Rigorous analysis of open microstrip lines of arbitrary cross-section in bound and leaky regimes," in *IEEE MTT-S Int. Microwave Symp. Dig.* (Long Beach, CA), 1989.

[10] K. S. Yee, "Numerical solution of initial boundary value problems involving Maxwell's equations in isotropic media," *IEEE Trans. Antennas Propagat.*, vol. AP-14, pp. 302–307, May 1966.

[11] A. Taflove and K. Umashankar, "Radar cross section of general three dimensional scatterers," *IEEE Trans. Electromagn. Compat.*, vol. EMC-25, pp. 433–440, Nov. 1983.
[12] D. H. Choi and W. J. R. Hoefer, "A graded mesh FD-TD algorithm for eigenvalue problems," in *Proc. European Microwave Conf.* (Rome), 1987, pp. 413–418.
[13] X. Zhang and K. K. Mei, "Time-domain finite difference approach to the calculation of the frequency-dependent characteristics of microstrip discontinuities," *IEEE Trans. Microwave Theory Tech.*, vol. 36, pp. 1775–1787, Dec. 1988.
[14] X. Zhang and K. K. Mei, "Time-domain calculation of microstrip components and the curve-fitting of numerical results," in *IEEE MTT-S Int. Microwave Symp. Dig.* (Long Beach, CA), 1989, pp. 313–316.
[15] C. J. Railton and J. P. McGeehan, "Analysis of microstrip discontinuities using the finite difference time domain technique," in *IEEE MTT-S Int. Microwave Symp. Dig.* (Long Beach, CA), 1989, pp. 1009, 1012.
[16] C. J. Railton and J. P. McGeehan, "Analysis of MMIC components including the effect of finite metallisation thickness," in *Proc. 20th European Microwave Conf.* (London) Sept. 1989, pp. 187–192.
[17] T. C. Edwards, *Foundations for Microwave Circuit Design*. New York: Wiley, 1981.
[18] K. Uchida, T. Noda, and T. Matsunagu, "New type of spectral-domain analysis of a microstrip line," *IEEE Trans. Microwave Theory Tech*, vol. 37, pp. 947–952, June 1989.

C. J. Railton (M'88) was born in Walsall, Staffordshire, England, in 1952. He received the B.Sc. degree (with honors) in physics with electronics from the University of London, London, England, in 1974 and the Ph.D. degree in electronic engineering from the University of Bath, Bath, England, in 1988.

During the period 1974–1984 he worked in the scientific civil service on a number of research and development projects in the areas of communications and signal processing. Between 1984 and 1987 he worked at the University of Bath on the mathematical modeling of boxed microstrip circuits. He is currently with the Communications Research Centre at the University of Bristol, Bristol, England, where he leads a group involved in the mathematical modeling and development of CAD tools for MMIC's, planar antennas, microwave heating systems, EMC, and high-speed logic.

Joseph P. McGeehan (M'83) obtained the degrees of B. Eng. (Hons) and Ph.D. in electrical and electronic engineering from the University of Liverpool, Liverpool, England, in 1967 and 1971 respectively.

From 1970 to 1972, he held the position of senior scientist at the Allen Clarke Research Centre, The Plessey Company Ltd., where he was primarily responsible for the research and development of high-power millimeter-wave GaAs sources and monolithic GaAs Gunn effect devices (two- and three-terminal) for ultra-high-speed logic. In September 1972 he was appointed to the academic staff of the University of Bath, Bath, England, where he led research groups in mobile communications, signal processing, and microwave techniques. Since July 1985, he has held the Chair of Communications Engineering in the Department of Electrical and Electronic Engineering, University of Bristol, Bristol, England, and is Director of the Centre for Communications Research there.

Dr. McGeehan is a member of a number of national and international committees in the field of communications.